

## Nonlocal host isotope effect in silicon: High-resolution spectroscopy of the $29\text{ cm}^{-1}$ oxygen vibrational line

K. Laßmann,<sup>1</sup> B. P. Gorshunov,<sup>1,2,3</sup> A. S. Prokhorov,<sup>2,3</sup> E. S. Zhukova,<sup>1,2,3</sup> P. S. Korolev,<sup>2,4</sup> V. P. Kalinushkin,<sup>2</sup>  
V. G. Plotnichenko,<sup>5</sup> N. V. Abrosimov,<sup>6</sup> P. G. Sennikov,<sup>7</sup> H.-J. Pohl,<sup>8</sup> and M. Dressel<sup>1</sup>

<sup>1</sup>*Physikalisches Institut, Universität Stuttgart, Pfaffenwaldring 57, 70550 Stuttgart, Germany*

<sup>2</sup>*A.M. Prokhorov General Physics Institute, Russian Academy of Sciences, Vavilov str. 38, 119991 Moscow, Russia*

<sup>3</sup>*Moscow Institute of Physics and Technology (State University), 141700, Dolgoprudny, Moscow Region, Russia*

<sup>4</sup>*M.V. Lomonosov Moscow State University, Faculty of Physics, 1-2 Leninskiye Gory, 119991 Moscow, Russia*

<sup>5</sup>*Fiber Optics Research Centre, Russian Academy of Sciences, Vavilov str. 38, 119333 Moscow, Russia*

<sup>6</sup>*Leibniz Institute for Crystal Growth, Max-Born-Straße 2, 12555 Berlin, Germany*

<sup>7</sup>*Institute of Chemistry of High-Purity Substances, Russian Academy of Sciences, Tropinin str. 49, 603950 Nizhny Novgorod, Russia*

<sup>8</sup>*Physikalisch-Technische Bundesanstalt, Bundesallee 100, 38116 Braunschweig, Germany*

(Received 23 August 2011; published 6 August 2012)

To investigate a possible host isotope effect on the local-mode-coupled low-energy two-dimensional motion of interstitial oxygen in silicon, we have measured the resonance parameters of the lowest transition of the  $29\text{ cm}^{-1}$  band of the Si-O-Si complex in three samples of natural silicon ( $^{\text{nat}}\text{Si}$ ) and in isotopically enriched  $^{28}\text{Si}$  and  $^{30}\text{Si}$  at temperatures between 5 and 50 K by means of coherent-source terahertz spectroscopy. At 5 K the resonance frequencies are  $29.220 \pm 0.003$ ,  $29.240 \pm 0.003$ , and  $28.820 \pm 0.006\text{ cm}^{-1}$  and the line widths are  $0.11 \pm 0.01$ ,  $0.10 \pm 0.01\text{ cm}^{-1}$ , and  $0.07 \pm 0.01\text{ cm}^{-1}$  for  $^{\text{nat}}\text{Si}$ ,  $^{28}\text{Si}$ , and  $^{30}\text{Si}$ , respectively; samples with similar oxygen content. The frequency of the resonance maximum in  $^{\text{nat}}\text{Si}$  is clearly downward shifted from that of  $^{28}\text{Si}$ , though 85.2% of the Si-O-Si in  $^{\text{nat}}\text{Si}$  consist of  $^{28}\text{Si}$  pairs. From this observation and the fact that not only the lines in the isotopically enriched samples but also in  $^{\text{nat}}\text{Si}$  can be fitted by single Lorentzians we conclude that shift and width of the  $^{\text{nat}}\text{Si}$ -resonance is not due to the Si isotopes in the Si-O-Si complex but to an average effect of the isotopically inhomogeneous lattice.

DOI: [10.1103/PhysRevB.86.075201](https://doi.org/10.1103/PhysRevB.86.075201)

PACS number(s): 71.55.Cn, 63.20.Pw

### I. INTRODUCTION

Oxygen is an unavoidable impurity in Czochralski-grown silicon with concentrations of about  $10^{18}\text{ cm}^{-3}$ . Depending, for instance, on the thermal history of the sample or the content of other impurities, oxygen will appear in a variety of complexes with wanted or unwanted technical relevance. In general oxygen occupies a bond-centred interstitial position on the  $\langle 111 \rangle$  axis between two Si neighbors.

The vibrational properties of such a Si-O-Si quasimolecule may be characterized by four fundamental modes:<sup>8</sup> A non-symmetric  $A_{2u}$  mode where the oxygen motion along the  $\langle 111 \rangle$  axis (large amplitude) is opposite to that of the two Si neighbors; a symmetric  $A_{1g}$  mode where only the two Si neighbors move along the  $\langle 111 \rangle$  axis oppositely to each other; a twofold degenerate  $E_u$  mode where only the two Si neighbors move in the plane perpendicular to the  $\langle 111 \rangle$  axis; and finally a so-called 2D LEAE (two-dimensional low-energy anharmonic excitation) mode, where only the oxygen moves (rotates/vibrates) in the plane perpendicular to the  $\langle 111 \rangle$  axis. The frequencies corresponding to the transitions from the ground to the first excited states of these modes are  $1136\text{ cm}^{-1}$  ( $A_{2u}$ ),  $648\text{ cm}^{-1}$  ( $A_{1g}$ ),  $517\text{ cm}^{-1}$  ( $E_u$ ), and  $29.2\text{ cm}^{-1}$  (2D LEAE); that is, the two high-frequency modes are local vibrational modes (LVMs), whereas the  $E_u$  mode is just below the maximum of the Si lattice phonons ( $524\text{ cm}^{-1}$ ) and finally the 2D LEAE or  $29\text{ cm}^{-1}$  mode lies in the linear range of the acoustic phonons. Due to transitions between higher excited states and due to nonlinear couplings between the various modes a multitude of lines is associated with the Si-O-Si complex.<sup>1-5</sup> (For a recent review, see Ref. 6.) The

(near) bond-centered interstitial position of oxygen in silicon was first established by Bosomworth *et al.*<sup>2</sup> They could fit the observed far-infrared transitions of the  $29\text{ cm}^{-1}$  mode by assuming that the oxygen is moving in a parabolic potential, which is perturbed by a small central hump without noticeable influence of the  $D_{3d}$  crystal potential. However, the  $^{16}\text{O}$  to  $^{18}\text{O}$  isotopic shift calculated with this model was distinctly larger than observed. This discrepancy was ascribed by the authors to the neglect of the contribution of Si to the motion.

To resolve the discrepancy, Yamada-Kaneta *et al.*<sup>7</sup> included the coupling of the  $29\text{ cm}^{-1}$  mode to the  $A_{2u}$  mode. They could not only consistently describe the oxygen isotopic shift but also the transitions from the  $A_{2u}$  zero-phonon states of the  $29\text{ cm}^{-1}$  band to the multiplets of the  $A_{2u}$  one-phonon states. This procedure has been extended later by including the coupling to the  $A_{1g}$  local mode. A set of energy levels could be obtained consistently describing all lines observed up to the  $A_{2u} + A_{1g}$  bands.<sup>8,9</sup> The quasilocalization of these LVMs of the Si-O-Si complex is evident from the fact that, correlated with  $^{28}\text{Si}$ -O- $^{28}\text{Si}$ -lines dominant in natural silicon, satellites are found that correspond to  $^{29}\text{Si}$ -O- $^{28}\text{Si}$  and  $^{30}\text{Si}$ -O- $^{28}\text{Si}$  complexes.<sup>2,10-13</sup> In isotopically enriched material, corresponding lines show narrowing and even slight shifts with respect to those in  $^{\text{nat}}\text{Si}$ . This has been discussed as an influence of beyond nearest neighbors or the lattice as a whole.<sup>12</sup>

Despite the coupling of the 2D LEAE mode to the LVMs, far-infrared (FIR) measurements<sup>2,14</sup> do not show an indication of a corresponding host isotope structure in  $^{\text{nat}}\text{Si}$ . It is therefore of interest to investigate the behavior of the 2D

LEAE in isotopically enriched [in the following, abridged by qmi (quasimonoisotopic<sup>6</sup>)] Si. Here we present a detailed experimental comparison of the  $29\text{ cm}^{-1}$  resonance in  $^{\text{nat}}\text{Si}$  and in qmi  $^{28}\text{Si}$  and  $^{30}\text{Si}$  employing a high-resolution coherent-source spectrometer.

## II. EXPERIMENTAL DETAILS

All single crystals investigated in this study were grown by Czochralski technique. To check for an influence of the oxygen concentration on the form and position of the resonance line in the case of  $^{\text{nat}}\text{Si}$ , we have measured three samples (1, 2, 3) with concentrations  $(5.7 \pm 0.2) \times 10^{16}\text{ cm}^{-3}$ ,  $(7.6 \pm 0.2) \times 10^{17}\text{ cm}^{-3}$ , and  $(1.5 \pm 0.2) \times 10^{18}\text{ cm}^{-3}$ , respectively. All three samples are dislocation-free and they contain impurities such as P or B in the range of  $10^{14}\text{ cm}^{-3}$ . The  $^{\text{nat}}\text{Si}$  dislocation-free phosphorus doped sample 2, for example, exhibits a room-temperature resistivity of  $5\ \Omega\text{cm}$ . The concentration of interstitial oxygen was determined from the intensity of the oxygen-related absorption peak located at  $1107\text{ cm}^{-1}$  measured at room temperature with a Fourier transform spectrometer in conformity with the ASTM standard F-1188.<sup>15</sup> A standard Si specimen with oxygen concentration less than  $5 \times 10^{15}\text{ cm}^{-3}$  served as reference. The oxygen content of the  $^{\text{nat}}\text{Si}$  specimen was  $(7.6 \pm 0.2) \times 10^{17}\text{ cm}^{-3}$ . The  $^{28}\text{Si}$  single crystal was grown in the frame of the Avogadro project,<sup>16</sup> the room temperature resistivity of the *p*-type crystal was  $4\ \Omega\text{cm}$ . The surface of the silica glass crucible was protected by a  $^{28}\text{SiO}_2$  layer to avoid dilution of highly enriched  $^{28}\text{Si}$ . Thus the enrichment of the starting material was basically not influenced and amounted to a value of 0.99994882(17). The oxygen concentration was determined at room temperature using the calibration factor  $3.14 \times 10^{17}\text{ cm}^{-3}$  for natural silicon and was found to be  $(5.5 \pm 0.2) \times 10^{17}\text{ cm}^{-3}$ , close to that in  $^{\text{nat}}\text{Si}$ , sample 2. The parameters of the  $^{30}\text{Si}$  single crystal are as follows: enrichment  $(99.769 \pm 0.060)\%$ ,  $[\text{O}] = (5.6 \pm 0.6) \times 10^{17}\text{ cm}^{-3}$ ,  $[\text{C}] = (5 \pm 2) \times 10^{16}\text{ cm}^{-3}$ ,  $[\text{B}] = 2.23 \times 10^{14}\text{ cm}^{-3}$ ,  $[\text{P}] = 5.12 \times 10^{14}\text{ cm}^{-3}$ .

For our spectroscopic investigations we employed a quasi-optical spectrometer<sup>17</sup> based on monochromatic continuous-wave radiation sources (backward-wave oscillators) that can be continuously frequency-tuned. It covers the frequency range from 30 GHz up to about 1.5 THz ( $1$  to  $50\text{ cm}^{-1}$ ). Utilizing a Mach-Zehnder interferometer, the complex transmission coefficient (transmission amplitude and phase) of plane-parallel samples can be measured and from that the dielectric response functions (complex conductivity, complex permittivity, etc.) can be determined.<sup>18</sup> For low-absorbing materials, the transmission spectra show oscillations (Fabry-Perot resonances) due to reflections of the radiation at the sample interfaces. In this case the real part of the dielectric permittivity  $\epsilon'$  can be determined from the positions of the interference maxima and the values of the imaginary part  $\epsilon''$  are found from the amplitude of the maxima.<sup>17</sup> The frequency resolution of the THz-spectrometer can be as high as  $\Delta\nu/\nu \approx 10^{-6}$  and the dynamical range is  $10^6$ . For the measurements presented below we used a spectral resolution of  $\Delta\nu \approx 0.005\text{ cm}^{-1}$  ( $\Delta\nu/\nu \approx 2 \times 10^{-4}$ ).

For the transmission measurements, samples with an area of approximately  $0.5$  to  $1\text{ cm}^2$  were prepared by polishing. The

thicknesses of the  $^{\text{nat}}\text{Si}$  samples 1, 2, and 3 were 4.86, 1.96, and 1.46 mm, respectively, that of  $^{28}\text{Si}$  was 2.59 mm and of  $^{30}\text{Si}$  1.03 mm. Data were taken in the spectral range from 28 to  $30\text{ cm}^{-1}$  at temperatures from 300 down to 5 K.

## III. RESULTS

In Fig. 1(a), spectra of the transmission at  $T = 5\text{ K}$  are shown for sample 3, i.e., the  $^{\text{nat}}\text{Si}$  sample with the highest oxygen concentration, and for both qmi samples. On the background of the interferometric oscillations, deep (note the logarithmic scale) minima are seen that correspond to the oxygen 2D LEAE resonances. Different depths of the minima are due to differences in sample thickness and oxygen concentration. The isotopic shifts of the lines of the qmi samples are indicated relative to the  $^{\text{nat}}\text{Si}$  resonance. Figure 1(b)

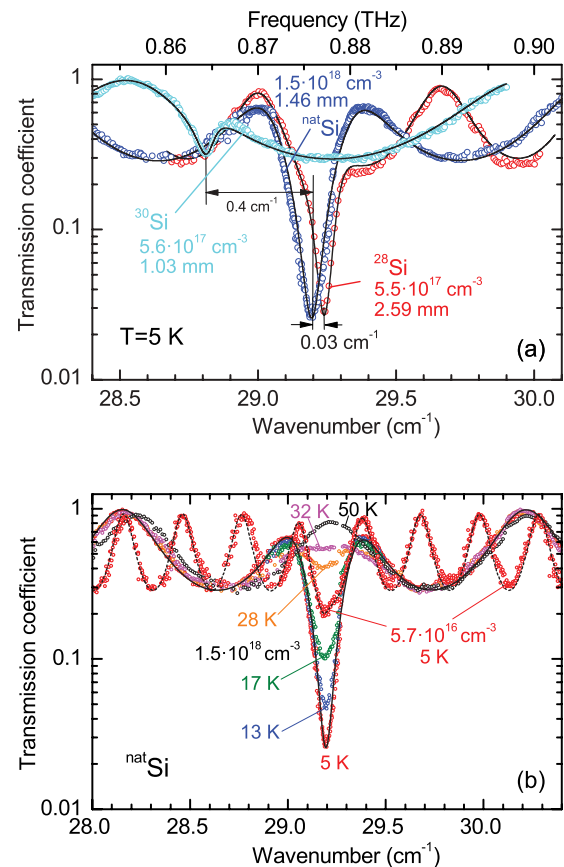


FIG. 1. (Color online) (a) Transmission spectra through plane-parallel silicon samples of natural  $^{\text{nat}}\text{Si}$  (sample 3), qmi  $^{28}\text{Si}$ , and qmi  $^{30}\text{Si}$  at  $T = 5\text{ K}$ . Interference of the radiation within the plane-parallel samples leads to broad oscillations in the background. The deep (note the logarithmic scale) minima are caused by the transition from the ground state to the next excited state of the  $29\text{ cm}^{-1}$  band. The dots correspond to experimental data; the lines represent the least square fits using Eq. (1), as described in the text. (b) For comparison the transmission through the  $^{\text{nat}}\text{Si}$ -samples 1 and 3 (i.e., with lowest and highest oxygen concentration) are shown. In the latter case, the temperature evolution of the resonance could be seen up to approximately 30 K but above about  $T = 22\text{ K}$  it was not possible to reliably register it. At 50 K no resonance could be identified in the transmission of sample 3.

shows the transmission for sample 1 at 5 K and the evolution of the resonance with temperature for sample 3. At 50 K no resonance can be identified in the transmission of sample 3. Our samples were too thin to observe at higher temperatures the weak 37, 43, or 48  $\text{cm}^{-1}$  lines that result from transitions starting from thermally excited to higher states of this band. With increasing temperature, the 29  $\text{cm}^{-1}$  minimum becomes weaker and broader. Above about 22 K it was not possible to reliably register the resonance.

For a quantitative characterization of the resonances and the temperature dependence of their parameters, we apply here the Kramers-Heisenberg formula for the atomic polarizability  $\alpha$ .<sup>18,19</sup> Defining  $\alpha$  by the proportionality  $p_{\text{ind}} = \alpha \epsilon_0 E$  between the local electric field  $E$  and the induced electric dipole moment  $p_{\text{ind}}$  we have for a molecule in state  $i$ :

$$\alpha_i(\omega, T) = \frac{q^2}{m^* \epsilon_0} \sum_j \frac{f_{ij}}{(\omega_{ij}^2(T) - \omega^2) - i\omega/\tau_{ij}(T)}, \quad (1)$$

where the transition oscillator strength  $f_{ij}$  is proportional to the product  $m^* \times \omega_{ij} \times$  square of the matrix element for dipolar transition from the initial state  $i$  to the final state  $j$  with energy difference  $E_j - E_i = \hbar \omega_{ij}(T)$ . The mass  $m^*$  introduced for a dimensionless definition of the oscillator strength is canceled by the prefactor of the sum and may be regarded here as a dummy parameter that reproduces the form of the classical Lorentz model of atomic polarizability.  $q$  is the charge effective for the excitation of the complex in the regarded mode. The lifetime broadening is described by  $1/\tau_{ij}(T)$  that includes the spontaneous emission and temperature-dependent broadening by phonons. From the polarizability given by Eq. (1) one obtains the dielectric susceptibility  $\chi_e = N\alpha$ :

$$\chi_e(\omega, T) = \sum_i N_i(T) \alpha_i(\omega, T) = \frac{q^2}{m^* \epsilon_0} \sum_i \sum_j N_i(T) \times \frac{f_{ij}}{[\omega_{ij}^2(T) - \omega^2] - i\omega/\tau_{ij}(T)}, \quad (2)$$

where  $\sum_i N_i(T) = N$ , the number density of the molecules in question. Limiting Eq. (2) to the range around the 29  $\text{cm}^{-1}$  resonance it reduces to the contribution of the ground state 1 and the next excited state 2:

$$\chi(\omega, T) = \frac{q^2}{m^* \epsilon_0} [N_1(T) - N_2(T)] \times \frac{f_{12}}{(\omega_{12}^2(T) - \omega^2) - i\omega/\tau(T)}. \quad (3)$$

Here,  $N_1$  and  $N_2$  take account of the twofold degeneracy of state 2 for transition probability (two final states in the transition 1 to 2) and its ‘‘twofold’’ occupancy for the transition 2 to 1. To calculate  $N_1(T)$  the equation  $\sum_i N_i(T) = N$  is used. Up to 30 K it is sufficient (within 1% deviation) to sum up the occupations of only the next four excited states.<sup>2,14</sup> The parameter

$$\begin{aligned} \phi_{12} &= \frac{q^2}{m^* \epsilon_0} [N_1(T) - N_2(T)] f_{12} \\ &= -i\chi(\omega = \omega_{12}, T) \frac{\omega_{12}(T)}{\tau(T)} \end{aligned} \quad (4)$$

is a measure of the area of the resonance and is called in the following the effective oscillator strength. Analogous definitions have been called ‘‘peak area’’<sup>14</sup> or ‘‘integrated absorption.’’<sup>6</sup> The temperature dependence of  $\phi_{12}$  involves the thermal occupation of the ground state depending on the energetic distance of the excited states. The parameters  $q$  and  $f_{12}$  may be of relevance for checking any model of the mode.

Using the Lorentzian expression of Eq. (3) for the transition, we calculated the complex dielectric permittivity and refractive index, and implemented it into the standard formula describing the transmission through a plane-parallel layer.<sup>18</sup> Fitting the raw data directly has been demonstrated to be superior compared to various intermediate steps taking the interference fringes within the substrate etc. into account before getting data of the dielectric properties.<sup>17</sup> Following this approach all experimental spectra were fitted using a least-square fit procedure; examples for  $T = 5$  K are shown by solid lines in Fig. 1. (Here and in the following the data are given in  $\text{cm}^{-1}$ , i.e., the eigenfrequency  $\nu_0 = \omega_{12}/(2\pi c)$ , the damping parameter  $\gamma = 1/(2\pi c\tau)$ ; and as a consequence the effective oscillator strength  $\phi_{12}$  in  $\text{cm}^{-2}$ .) It turns out that the absorption lines of all samples of  $^{\text{nat}}\text{Si}$  and of qmi  $^{28}\text{Si}$  and  $^{30}\text{Si}$  can be fitted by single Lorentzians. From these fitting curves we obtain the graphs of Figs. 2(a) and 2(b) showing the imaginary part of

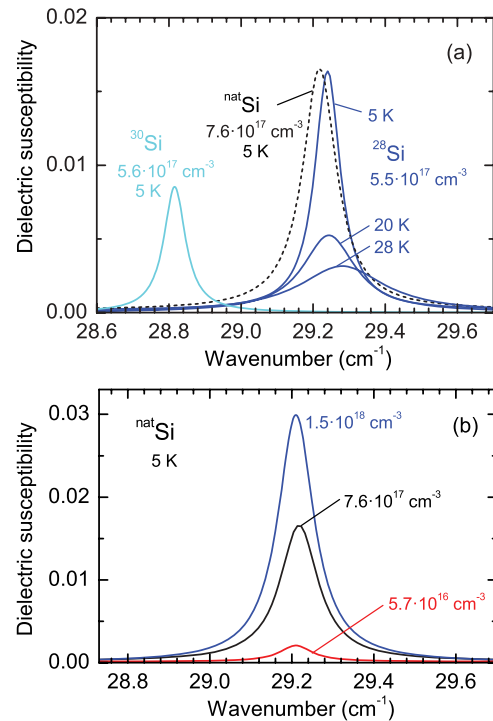


FIG. 2. (Color online) (a) Spectra of the imaginary part of the dielectric susceptibility of the qmi  $^{28}\text{Si}$  and  $^{30}\text{Si}$  as well as of  $^{\text{nat}}\text{Si}$  sample 2 at 5 K. The center frequency of the latter resonance is slightly downshifted relative to  $^{28}\text{Si}$  by  $\Delta\nu_0 = 0.02 \text{ cm}^{-1}$  and it is considerably broader. For the  $^{28}\text{Si}$  sample two spectra at higher temperatures are given showing broadening and shift of the resonance. The spectra are obtained by fitting the optical transmission by expression (3) as presented in Fig. 1 and described in the text. (b) The three spectra of the  $^{\text{nat}}\text{Si}$  samples 1, 2, and 3 demonstrate that in this range of oxygen concentration there is no significant variation of position and line width of the resonance.

the dielectric susceptibility of the samples at 5 K. In Fig. 2(a) the dielectric susceptibility of the qmi samples  $^{28}\text{Si}$  and  $^{30}\text{Si}$  is shown in comparison to that of the  $^{\text{nat}}\text{Si}$  sample 2, which has about the same oxygen content as the two qmi samples. The center frequency of the  $^{\text{nat}}\text{Si}$  resonance is slightly downshifted relative to  $^{28}\text{Si}$  by  $\Delta\nu_0 = 0.02 \text{ cm}^{-1}$  and is distinctly broader than the line width of both qmi samples. Astonishingly, the dielectric susceptibility of  $^{30}\text{Si}$  is about a factor of two smaller than that of the two other samples with nearly the same oxygen content. For the  $^{28}\text{Si}$  sample two spectra at higher temperatures are given showing the broadening and shift of the resonance. The spectra of the  $^{\text{nat}}\text{Si}$  samples 1, 2, and 3 in Fig. 2(b) demonstrate that in this range of oxygen concentration there is no significant variation of position and line width of the resonance. For the resonance positions we have 29.21, 29.22, and 29.19  $\text{cm}^{-1}$  with line widths 0.10  $\text{cm}^{-1}$ , 0.11  $\text{cm}^{-1}$ , and 0.11  $\text{cm}^{-1}$  for samples 1, 2, and 3, respectively. Previous authors obtained slightly different results for position, line width, and resolution, respectively:

$\nu_0 = 29.25 \text{ cm}^{-1}$ ,  $\gamma = 0.09 \text{ cm}^{-1}$ ,  $\Delta\nu = 0.01 \text{ cm}^{-1}$ ,  $[O_i] = 2 \times 10^{17} \text{ cm}^{-3}$  (Fourier transform),<sup>14</sup>  
 $\nu_0 = 29.29 \text{ cm}^{-1}$ ,  $\gamma = 0.15 \text{ cm}^{-1}$ ,  $\Delta\nu = 0.05 \text{ cm}^{-1}$ ,  $[O_i] = 2.5 \times 10^{15} \text{ cm}^{-3}$  (phonon spectroscopy),<sup>20</sup>  
 $\nu_0 = 29.2 \text{ cm}^{-1}$ ,  $\gamma = 0.13 \text{ cm}^{-1}$ ,  $\Delta\nu = 0.12 \text{ cm}^{-1}$ ,  $[O_i] = 1.8 \times 10^{18} \text{ cm}^{-3}$  (FIR laser),<sup>21</sup>  
 $\nu_0 = 29.2 \text{ cm}^{-1}$ ,  $\gamma = 0.09 \text{ cm}^{-1}$ ,  $\Delta\nu = 0.01 \text{ cm}^{-1}$ ,  $[O_i] = 6 \times 10^{17} \text{ cm}^{-3}$  (backward wave oscillator),<sup>22</sup>  
 $\nu_0 = 29.3 \text{ cm}^{-1}$ ,  $\gamma = 0.2 \text{ cm}^{-1}$ ,  $\Delta\nu = 0.2 \text{ cm}^{-1}$ ,  $[O_i] = 7 \times 10^{17} \text{ cm}^{-3}$  (Fourier transform).<sup>2</sup>

The parameters  $\nu_0$ ,  $\gamma$ , and  $\phi_{12}$  and their temperature dependencies are plotted in Fig. 3 for all samples. In Table I we list the parameter values obtained at  $T = 5 \text{ K}$ .

## IV. DISCUSSION

### A. Spectra at 5 K

We may summarize our findings as follows: (i) The resonance frequency decreases with increasing ‘‘average’’ Si-mass. (ii) All resonances can be well fitted by single Lorentzians. (iii) The line width of the  $^{\text{nat}}\text{Si}$  resonance does not depend on the oxygen concentration and is somewhat broader than that of the qmi Si. We shall discuss two alternatives that may contribute to the observed host isotope effect on the 29  $\text{cm}^{-1}$  oxygen resonance:

TABLE I. Parameters obtained from Lorentzian fits of the 29  $\text{cm}^{-1}$  resonance in three samples of  $^{\text{nat}}\text{Si}$  and in  $^{28}\text{Si}$  and  $^{30}\text{Si}$  single crystals: eigenfrequency  $\nu_0$ , effective oscillator strength  $\phi_{12}$  [see Eq. (4) for definition], and damping parameter  $\gamma$ . The temperature  $T$  of the measurements and the oxygen concentration  $[O_i]$  are also indicated.

	$T$ (K)	$[O_i]$ ( $10^{17} \text{ cm}^{-3}$ )	$\phi_{12}$ ( $\text{cm}^{-2}$ )	$\nu_0$ ( $\text{cm}^{-1}$ )	$\gamma$ ( $\text{cm}^{-1}$ )
$^{\text{nat}}\text{Si}$ -1	5	$0.57 \pm 0.02$	0.067	$29.21 \pm 0.02$	$0.10 \pm 0.05$
$^{\text{nat}}\text{Si}$ -2	5.5	$7.6 \pm 0.2$	0.692	$29.220 \pm 0.003$	$0.11 \pm 0.01$
$^{\text{nat}}\text{Si}$ -3	5	$15 \pm 2$	1.17	$29.21 \pm 0.01$	$0.11 \pm 0.01$
$^{28}\text{Si}$	5.5	$5.5 \pm 0.2$	0.513	$29.240 \pm 0.003$	$0.10 \pm 0.01$
$^{30}\text{Si}$	5.5	$5.6 \pm 0.6$	0.236	$28.820 \pm 0.006$	$0.07 \pm 0.01$

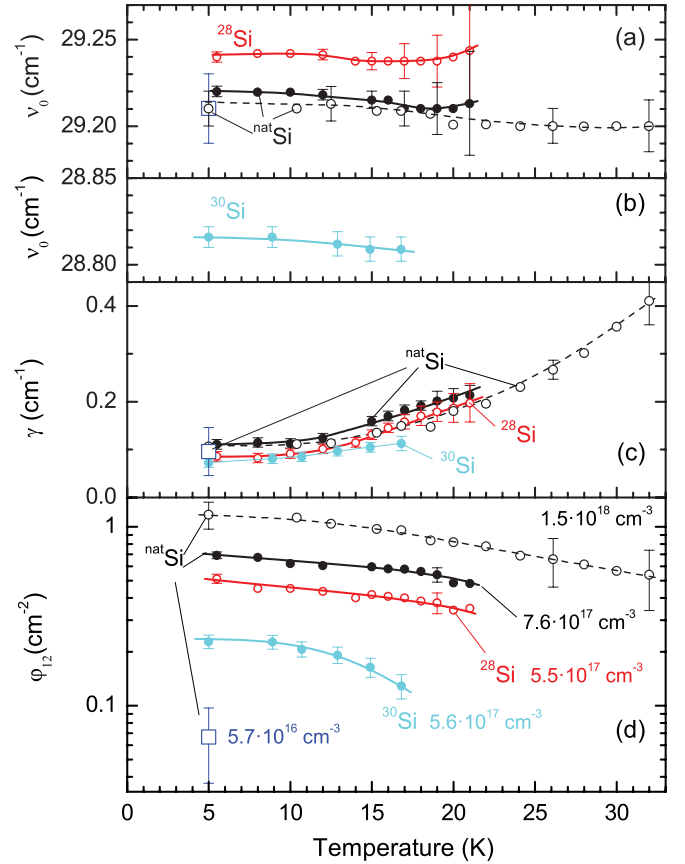


FIG. 3. (Color online) Temperature dependencies of parameters of the 29  $\text{cm}^{-1}$ -resonance of interstitial oxygen in  $^{28}\text{Si}$ ,  $^{30}\text{Si}$ , and  $^{\text{nat}}\text{Si}$ : (a) and (b) eigenfrequency  $\nu_0$ , (c) damping parameter  $\gamma$ , and (d) effective oscillator strength  $\phi_{12}$ .

### 1. Local isotope effect

It is mainly the isotopic mass of the two Si partners in the Si-O-Si complex that determines the host isotopic shifts of the line positions.

This is the situation dominant in the LVMs  $A_{2u}$  and  $A_{1g}$ . As a consequence of a local host isotope effect, the concerning resonances of the Si-O-Si complex in  $^{\text{nat}}\text{Si}$  are made up of all Si-isotopic pairings. Since  $^{\text{nat}}\text{Si}$  contains 92.23% of  $^{28}\text{Si}$ , 4.67% of  $^{29}\text{Si}$ , and 3.10% of  $^{30}\text{Si}$ , the most important components of the absorption are due to the constituents  $^{28}\text{Si}$ - $^{28}\text{Si}$  (probability 85.06%),  $^{28}\text{Si}$ - $^{29}\text{Si}$  (8.61%), and  $^{28}\text{Si}$ - $^{30}\text{Si}$  (5.72%), that is, the mixed pairings 28-29 and



28-30 are less probable than 28-28 by a factor of 0.100 and 0.066, respectively. For large enough shifts between these components there will be three resolvable lines with relative intensities corresponding to their probabilities. This is the case for the  $A_{1g}$  and  $A_{2u}$  transitions at 648 and 1136  $\text{cm}^{-1}$  and also for the  $A_{1g} + A_{2u}$  combination at 2273  $\text{cm}^{-1}$  (see, e.g., Refs. 2,10–13). Comparison of the  $A_{2u}$  transitions in  $^{\text{nat}}\text{Si}$  with those in qmi Si samples<sup>12,13</sup> shows that the  $^{28}\text{Si-O-}^{30}\text{Si}$  component in  $^{\text{nat}}\text{Si}$  is about midway between the  $^{28}\text{Si}$  and the  $^{30}\text{Si}$  line in the qmi crystals and the  $^{28}\text{Si-O-}^{29}\text{Si}$  is about midway between the  $^{28}\text{Si-O-}^{28}\text{Si}$  and the  $^{28}\text{Si-O-}^{30}\text{Si}$  components in  $^{\text{nat}}\text{Si}$ . Remarkably, the  $A_{2u}$   $^{28}\text{Si-O-}^{28}\text{Si}$ -line observed in  $^{\text{nat}}\text{Si}$  is at the same position but, though well resolved, is broader by 0.18  $\text{cm}^{-1}$  than in the qmi  $^{28}\text{Si}$  sample.

For both Si-O-Si LVMs a local isotope effect has a clear meaning, since the Si partners are essentially involved in the vibrational motion. This is not the case for the 29  $\text{cm}^{-1}$  mode where only the oxygen is moving. However, a local effect—if measured—would not necessarily mean that the Si-partners take part in the slow motion of the oxygen. Corresponding to the idea of a nonlinear coupling between LVMs and the 29  $\text{cm}^{-1}$  band<sup>7</sup> the fast motion will—depending on the mass of the two partners—change the potential for the slow oxygen motion and thus change the position of the states [see Eq. (9) of Ref. 7].

If this coupling would show up as a local host isotope effect in the 29  $\text{cm}^{-1}$  resonance in  $^{\text{nat}}\text{Si}$  we would expect an analogous dependence of the isotope shifts as for  $A_{2u}$ ; i.e., from the observed difference in line position between the  $^{28}\text{Si}$  and  $^{30}\text{Si}$  samples, the  $^{28}\text{Si-O-}^{29}\text{Si}$  component should be seen at 29.12  $\text{cm}^{-1}$  and the  $^{28}\text{Si-O-}^{30}\text{Si}$  component at 29.03  $\text{cm}^{-1}$ . As shown in Fig. 4, such a combination deviates distinctly from the experimental result.<sup>23</sup>

As a measure of the contribution of a local host isotope effect to the vibrational resonance we compare the relative shift between the  $^{28}\text{Si}$  and  $^{30}\text{Si}$  resonances of the three modes in question. We get (in units of  $\text{cm}^{-1}$ ) for the

$$2\text{D LEAE } (29.24 - 28.82)/29.24 = 0.014.$$

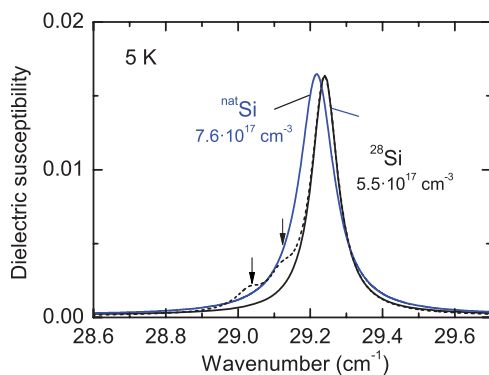


FIG. 4. (Color online) Spectra of the imaginary part of the dielectric susceptibility of the qmi  $^{28}\text{Si}$  and  $^{\text{nat}}\text{Si}$ . The broken line is calculated with the assumption that the shifts of the  $^{28}\text{Si}$  and  $^{30}\text{Si}$  resonances are determined by a local host isotope effect resulting from the anharmonic coupling of the 2D LEAE mode to  $A_{2u}$ . The two humps indicated by arrows would then be the 28-29 and 28-30 resonances to appear in  $^{\text{nat}}\text{Si}$ .

$$A_{2u} (1136.4 - 1129.1)/1136.4 = 0.006 \text{ (Ref. 12)}$$

$$A_{1g} (648.1 - 629)/648.1 = 0.03 \text{ (Ref. 28).}$$

We see that the relative shift of 2D LEAE lies between that of the two LVMs. It is plausible that the relative host isotope shift is largest for  $A_{1g}$  since the oxygen motion in this mode is near to negligible as compared to that of the Si-neighbors. In the  $A_{2u}$  mode, both Si and O motion are important with a large amplitude of the oxygen (see Fig. 6 of Ref. 12), so it is not surprising that the relative shift is much smaller than in  $A_{1g}$ . However, for the 2D LEAE resonance an even smaller difference is expected since, as mentioned above, the resonance can be modeled by a potential for a motion of the oxygen alone.<sup>2</sup> (The relative oxygen isotope shift of the 29  $\text{cm}^{-1}$  resonance is nearly a factor 2 larger than that of  $A_{2u}$ .) The large 2D LEAE relative host isotopic shift between  $^{28}\text{Si}$  and  $^{30}\text{Si}$  may be taken as an indication of a host isotope effect different to that of the two LVMs. We conclude from the foregoing that a local host isotope effect cannot be deduced from our experimental data. It may well be that the influence of the  $A_{2u}$  local host isotope effect on the 29  $\text{cm}^{-1}$  resonance is too weak to be seen since for  $A_{2u}$  the Si isotope shift is much smaller than the oxygen isotope shift.<sup>29</sup>

## 2. Nonlocal isotope effect

The change of the (average) isotopic mass of the host will involve the lattice as a whole by the change of some properties such as lattice constant or phonon spectrum to mention only the two that may be of relevance here.

Since the 2D LEAE resonance lies in the linear range of the acoustic phonon spectrum (where the stress dependence is small<sup>30,31</sup>) and since the coupling of the resonance to the phonons is rather weak<sup>32</sup> we do not expect a noticeable host isotope effect due to a change in the vibration-phonon interaction. (For a recent review on isotope effects on the optical spectra of semiconductors, see Ref. 33.)

A change of the lattice constant can be understood as an effective strain that changes the configuration of the Si-O-Si complex and by that the resonance frequencies as in the case of hydrostatic pressure.<sup>34</sup> This type of host isotope effect may be dominant in the case of the 2D LEAE vibration. If so, one would expect in qmi material shifted lines with lifetime determined line widths, whereas for  $^{\text{nat}}\text{Si}$  the line width may be inhomogeneously broadened by the isotopic fluctuations of the lattice constant or the internal strains due to the difference of the apparent radii of the different isotopes due to the anharmonicity. According to Stoneham<sup>35</sup> point defects will induce a broadening with Lorentzian line shape proportional to the relative difference of impurity and host radii. Because of the statistical averaging we would not expect a broadening that is structured by the 28-29 and 28-30 components in  $^{\text{nat}}\text{Si}$  as for the local host isotope effect.

To estimate the effect of a change  $\Delta a/a$  of the lattice constant  $a$  we identify this change with the strain component  $e_{111}$  and relate this to the component  $\sigma_{111}$  of the externally applied stress by help of Young's modulus  $Y_{111}$  for the  $\langle 111 \rangle$  direction:  $Y_{111} = -\sigma_{111}/\epsilon_{111} = \sigma_{111}/(\Delta a/a)$ .

With  $Y_{111} = 190 \text{ GPa}$ <sup>36</sup> and  $\Delta a/a = -6 \times 10^{-5}$  for a difference of 2AMU,<sup>37</sup> i.e., between the  $^{28}\text{Si}$  and the  $^{30}\text{Si}$  resonances, we obtain  $\sigma_{111} = 11.3 \text{ MPa}$ . This has to be

compared with the experimentally determined line shift due to an externally applied stress. For stress in the  $\langle 111 \rangle$  direction, Bosomworth *et al.*<sup>2</sup> get for the shift  $\Delta\nu = -1.14 \times 10^{-8} \text{ cm}^{-1}/\text{Pa}$ . A similar value ( $-1.07 \times 10^{-8} \text{ cm}^{-1}/\text{Pa}$ ) has been measured much later by phonon spectroscopy<sup>38</sup> with linear dependence measured between 46 and 83 MPa (Bosomworth *et al.* at 180 MPa), that is, we can apparently extrapolate linearly down to 11.3 MPa.

For the stress of 11.3 MPa, we thus obtain  $\Delta\nu = -0.13 \text{ cm}^{-1}$ , i.e., a factor of three smaller than the measured  $-0.42 \text{ cm}^{-1}$ . In view of the simple identification of  $\Delta a/a$  with the stress-induced strain, this discrepancy does not necessarily exclude a contribution of the change in lattice constant to a nonlocal host isotope effect.

As regards the broadening of the  $^{\text{nat}}\text{Si}$  resonance, it is clear that  $\text{O}_i$  as the dominant impurity in  $^{\text{nat}}\text{Si}$  cannot be the cause. This is evident from the fact that the oxygen content of both qmi samples and of  $^{\text{nat}}\text{Si}$  sample 2 are nearly the same. Also the three samples of  $^{\text{nat}}\text{Si}$  with their different contents of  $\text{O}_i$  show all nearly the same line width.

Common to all these  $^{\text{nat}}\text{Si}$ -samples is a percentage of the isotopes  $^{29}\text{Si}$  and  $^{30}\text{Si}$  in a  $^{28}\text{Si}$  lattice. We assume that the  $^{28}\text{Si}$  lattice is perturbed by internal strains generated by the extra isotopes due to their deviating radii given by  $\Delta a/a$ . As mentioned before, a Lorentzian broadening of a resonance may be due to internal strains generated by point defects due to the fact that their effective radius deviates from that of the lattice.<sup>35</sup>

To estimate their effect on line broadening, we take profit from analogous previous investigations of the distribution of internal strains due to interstitial oxygen  $\text{O}_i$  and substitutional carbon  $\text{C}_s$  as point defects in Si. The strain-induced perturbation of the fourfold degenerate acceptor ground state in Si:B was determined by ultrasonic resonance spectroscopy<sup>40</sup> in the GHz range or by measuring the broadening of the EPR<sup>39</sup> or APR<sup>41</sup> resonances depending on the concentration  $\text{O}_i$  and  $\text{C}_s$ .

We scale the values of the three relevant parameters obtained by those measurements to the present problem, namely:

- (1) concentration  $n$  of the impurity,
- (2) the relative difference of radii between impurity and host  $[\Delta R/R = (R_I - R_{\text{Si}})/R_{\text{Si}}]$ ,
- (3) the stress dependence of the resonance,

and compare the extrapolated line width with the observed.

For the acoustic experiments Monte-Carlo simulations of the distribution of the strain splittings have been made<sup>41</sup> taking into account the anisotropy of the cubic crystal.<sup>39</sup> Lorentzian distributions were obtained with line widths in good agreement with the experimental results, especially at higher defect concentrations.<sup>40,41</sup> At smaller concentrations, a residual Gaussian becomes more and more apparent, not depending on the concentration of the acceptor boron in the  $10^{15} \text{ cm}^{-3}$  to  $10^{17} \text{ cm}^{-3}$  range<sup>39-41</sup> and distinctly broader than the lifetime broadening obtained from resonance saturation.<sup>40,42</sup>

For scaling we take the following parameters from the GHz experiments:

- (1) concentration of  $\text{C}_s$ ,  $n_C = 10^{17} \text{ cm}^{-3}$ ,
- (2)  $\Delta R/R = (R_C - R_{\text{Si}})/R_{\text{Si}} = (77 - 117) \text{ pm}/117 \text{ pm} = -0.34$ ,

(3)  $\Delta\nu/\sigma_{111} = -2.4 \times 10^{-7} \text{ cm}^{-1}/\text{Pa}$ ,<sup>41</sup> and the corresponding line width  $\gamma = 0.46 \text{ GHz} = 1.5 \times 10^{-2} \text{ cm}^{-1}$  (from Monte-Carlo simulations).<sup>41</sup>

The analogous parameters of the  $^{\text{nat}}\text{Si}$  resonance are:

- (1)  $n_{29} = 23.5 \times 10^{20} \text{ cm}^{-3}$ ,  $n_{30} = 15.5 \times 10^{20} \text{ cm}^{-3}$ ,
- (2)  $(\Delta R/R)_{29} = -3 \times 10^{-5}$ ,  $(\Delta R/R)_{30} = -6 \times 10^{-5}$
- (3)  $\Delta\nu/\sigma_{111} = -1.14 \times 10^{-8} \text{ cm}^{-1}/\text{Pa}$ .

We add the strains generated by the two isotopes by  $n_{29}(\Delta R/R)_{29} + n_{30}(\Delta R/R)_{30} = -1.64 \times 10^{17} \text{ cm}^{-3}$ . Thus, we obtain:  $\gamma_{\text{O}_i} = (1.64 \times 10^{17}/0.34 \times 10^{17})(-1.14 \times 10^{-8}/-2.4 \times 10^{-7})1.5 \times 10^2 \text{ cm}^{-1} = 3.4 \times 10^{-3} \text{ cm}^{-1}$ . The observed broadening, that is the difference between the line widths of  $^{\text{nat}}\text{Si}$  and the  $^{28}\text{Si}$ , is  $0.01 \text{ cm}^{-1}$ . This is a factor of three larger than the extrapolated value. As a result, both parameters,  $^{30}\text{Si}$  line shift and  $^{\text{nat}}\text{Si}$  line broadening, are larger by a factor of three than the estimated values based on the isotopic shift of the lattice constant. Whether this discrepancy is owed to the rather straightforward arguing or indicates an only small contribution of nonlocal isotope induced strain on the Si-O-Si complex is not easy to judge for now.

As regards the LVMs, a nonlocal host isotope effect due to  $\Delta a/a$  will be smaller since the stress-induced resonance shift is much smaller than for the 2D LEAE resonance.<sup>2</sup> It would show up as a slight broadening of the resonance in  $^{\text{nat}}\text{Si}$  and as an additional shift of the resonance in qmi samples. In Ref. 12, where the host isotope effect of LVMs has been investigated, a broadening of the basic  $A_{2u}$  resonance has indeed been found. On the other hand, an extra shift of the resonance in 29-29 and 30-30 material would be only noticed if there were a precise theory of the shift due to the local host isotope effect. However, since the 29-29 sample in Ref. 12 contained 2.17% of  $^{28}\text{Si}$  the 28-29 resonance could be observed in both the  $^{\text{nat}}\text{Si}$  and the qmi  $^{29}\text{Si}$  sample: This resonance in the latter was down-shifted by  $0.07 \text{ cm}^{-1}$ , that is a relative shift of only 0.00006 referred to  $^{\text{nat}}\text{Si}$  where in this context the lattice may be regarded as a perturbed 28 lattice. The authors have discussed these observations in terms of isotopic mass disorder and change of lattice constant. In contrast to 2D LEAE, a change of frequency of the  $A_{2u}$  mode will meet a change in the three-phonon density of states, changing the decay of the vibration and, thus, the lifetime determined line width, which complicates the discussion of the line width of the resonance.<sup>43</sup> As a whole, these observations in the case of  $A_{2u}$  seem to conform with our interpretation of the host isotope effect of the 2D LEAE resonance.

## B. Temperature dependence of the parameters

In  $^{\text{nat}}\text{Si}$  the temperature dependencies of the lower resonances in the  $29 \text{ cm}^{-1}$  band have been measured by Yamada-Kaneta<sup>14</sup> between 7 and 47 K. As mentioned above we were not able to reliably register the resonances above  $T \approx 22 \text{ K}$ , since our samples were not thick enough to measure small absorptions.

As seen from Figs. 3(a) and 3(b), the resonance frequencies of all samples remain constant up to approximately 10 K and then decrease slightly. In the case of  $^{\text{nat}}\text{Si}$  and  $^{28}\text{Si}$ , there is an indication of an increase above  $T \approx 19 \text{ K}$ . However, in this range of temperature the precision is not good enough to say whether this change is real. In Ref. 14 for the absorption

maxima at 7 K and at 37 K the values of 29.25 and 29.27  $\text{cm}^{-1}$ , respectively, are given.

Figure 3(c) shows that at 5 K the two higher doped  $^{\text{nat}}\text{Si}$  samples have the same line width, which is somewhat larger than the line width of both qmi samples. At higher temperatures the curves of  $^{28}\text{Si}$  and of the  $^{\text{nat}}\text{Si}$  sample 3 run together. The deviation of the  $^{\text{nat}}\text{Si}$  sample 2 and of  $^{30}\text{Si}$  is not clear. In this temperature range the line width starts to be determined by the interaction with acoustical phonons in the linear range of dispersion at these frequencies. The temperature dependence of the homogeneous line width  $\gamma$  has been calculated by Yamada-Kaneta.<sup>32</sup> In his calculation of the probability of phonon transitions between the states of the band, Yamada-Kaneta found that the transition probability between ground and next excited state is rather weak. This, together with the small thermal occupation of the higher state explains the long relaxation time of the first excited state, i.e., the small line width at the lowest temperatures. With increasing temperature, new relaxation channels open by two-phonon processes via the relatively closely lying higher states. (A schematic diagram of the strength of the various one-phonon transition probabilities between the states of this band is given in Ref. 32.) Our measurements are in good agreement with these findings, as far as can be judged from Fig. 2 in Ref. 32.

The effective oscillator strength  $\phi_{12}$  [Fig. 3(d)] at  $T = 5$  K should be proportional to the concentration of  $O_i$  in the sample since only the ground state is occupied. This need not be true if one of the parameters  $q$  and  $f_{12}$  will also differ for different samples. To compare we shall take the ratio  $(N/(10^{16} \text{ cm}^{-3})/(\phi_{12}/\text{cm}^{-2}))$ , which should be the same for samples of the same type and increase with decreasing  $q^*$  and  $f_{12}$ . We measure for  $^{\text{nat}}\text{Si}$ -3 and  $^{\text{nat}}\text{Si}$ -2 with concentrations of 150 and  $76 \times 10^{16} \text{ cm}^{-3}$ , respectively, similar ratios, namely 132.7 and 126.7. The ratio for the  $^{28}\text{Si}$  sample (concentration  $57 \times 10^{16} \text{ cm}^{-3}$ ) is somewhat smaller: 114. On the other hand, the ratio for  $^{30}\text{Si}$  (concentration  $56 \times 10^{16} \text{ cm}^{-3}$ , nearly identical to that of  $^{28}\text{Si}$ ), is distinctly larger: 237.<sup>45</sup> One might say that the ratio increases with increasing (average) mass of the Si host. The temperature dependence of the effective oscillator strength  $\phi_{12}$  is determined by the thermal occupation of the involved states. For comparison we take the ratio  $\phi_{12}(5 \text{ K})/\phi_{12}(21 \text{ K}) = [N_1(5 \text{ K}) - N_2(5 \text{ K})]/[N_1(21 \text{ K}) - N_2(21 \text{ K})]$ , assuming that the parameters  $q$  and  $f_{12}$  do not depend on temperature. Including the four next higher states to determine the occupation of the ground and first excited states we get  $2/1.34 = 1.49$ . The experimental values are for  $^{\text{nat}}\text{Si}$ -3:  $1.13/0.83 = 1.35$ , for  $^{\text{nat}}\text{Si}$ -2:  $0.7/0.5 = 1.40$ , and for  $^{28}\text{Si}$ :  $0.5/0.34 = 1.47$ . From Fig. 3 in Ref. 14, showing the temperature dependence of the “peak area,” we take  $0.98/0.65 = 1.51$ , so there is altogether good agreement for these three samples.

However, it is clear from the diagram that  $\phi_{12}$  of  $^{30}\text{Si}$  decreases much faster with temperature than the other samples. Extrapolating linearly from 15 to 21 K we obtain

$\phi_{12}(5\text{K})/\phi_{12}(21\text{K}) = 3.37$ , whereas the calculated ratio is only 1.52 when one reduces the energy of all excited states relative to the ground state by the same factor as for the first excited state as determined by the resonance shift  $28.22 \text{ cm}^{-1}/29.22 \text{ cm}^{-1} = 0.986$ . More experimental data are needed to discuss and understand this discrepancy. It would be helpful to be able to measure the resonances occurring at higher temperatures especially in  $^{30}\text{Si}$  but also in  $^{29}\text{Si}$ , i.e., with thicker samples.

## V. SUMMARY

We have presented a detailed experimental comparison of the 29  $\text{cm}^{-1}$  mode in  $^{\text{nat}}\text{Si}$  and in qmi  $^{28}\text{Si}$  and  $^{30}\text{Si}$ , employing a high-resolution coherent-source spectrometer. We find a host-isotope effect that is relatively large in view of the fact that this low-energy mode (2D LEAE mode) can be understood by an oxygen motion perpendicular to the Si-O-Si axis; relatively large also when compared with the host isotope effects of the  $A_{1g}$  and  $A_{2u}$  modes of the Si-O-Si complex, where the Si motion is an essential part of the vibration of the complex. In contrast to the local host isotope effect given by the mass of two silicon atoms in these high-energy modes, the 2D LEAE line in  $^{\text{nat}}\text{Si}$  does not show a structure corresponding to the resonances of the different pairings of the three Si isotopes in  $^{\text{nat}}\text{Si}$ . Though the line width is larger than for  $^{28}\text{Si}$  and  $^{30}\text{Si}$ , the line is nevertheless symmetric and can be fitted by a single Lorentzian. From this we conclude that the observed host isotope effect is not due to a local isotope effect within the Si-O-Si complex but is an effect of the lattice as a whole. We have given estimates by analogy of previous investigations and with the assumption that the isotopic change of the lattice constant is a measure of the strains acting on the Si-O-Si complex. The values thus obtained are distinctly smaller than the observed. Additional measurements with  $^{29}\text{Si}$ , for instance, may help for a better understanding of the host isotope effect of the 2D LEAE mode. In this context, it should be interesting to reconsider the host isotope effect of the 2D LEAE mode of the Ge-O-Ge complex in Ge, previously investigated by phonon spectroscopy, to see whether it can be understood by a nonlocal host isotope effect alone. Also there, some specific high-resolution experiments may help to clarify the situation.

## ACKNOWLEDGMENTS

The authors thank L. I. Khirunen for her help in determining the oxygen content in  $^{28}\text{Si}$  and V. I. Torgashev for useful discussions. We thank Gabi Untereiner for her skilled help with the preparation of the  $^{\text{nat}}\text{Si}$  samples. We acknowledge helpful communications with M. D. McCluskey, B. Pajot, A. M. Stoneham, and H. Yamada-Kaneta. The work was supported by the RAS program for fundamental research “Problems of Radiophysics,” ISTC Project No. 3736, and RFBR Grant No. 10-08-01323-a.

<sup>1</sup>W. Kaiser, P. H. Keck, and C. F. Lange, *Phys. Rev.* **101**, 1264 (1956).

<sup>2</sup>D. R. Bosomworth, W. Hayes, A. R. L. Spray, and G. D. Watkins, *Proc. R. Soc. London A* **317**, 133 (1970).

<sup>3</sup>T. Hallberg, L. I. Murin, J. L. Lindström, and V. P. Markevich, *J. Appl. Phys.* **84**, 2466 (1998).

<sup>4</sup>L. I. Murin, V. P. Markevich, T. Hallberg, and J. L. Lindström, *Solid State Phenomena* **69–70**, 309 (1999).

- <sup>5</sup>H. Yamada-Kaneta, *Physica B* **302–303**, 172 (2001).
- <sup>6</sup>B. Pajot and B. Clerjoud, *Optical Absorption of Impurities and Defects in Semiconducting Crystals: II. Electronic Spectra of Deep Centres and Vibrational Spectra*, Springer Series in Solid-State Sciences 169 (Springer, Berlin, Heidelberg, 2012).
- <sup>7</sup>H. Yamada-Kaneta, C. Kaneta, and T. Ogawa, *Phys. Rev. B* **42**, 9650 (1990).
- <sup>8</sup>H. Yamada-Kaneta, *Physica B* **308–310**, 309 (2001).
- <sup>9</sup>H. Yamada-Kaneta, *Phys. Status Solidi C* **0**, 673 (2003).
- <sup>10</sup>B. Pajot and J. P. Deltour, *Infrared Phys.* **7**, 197 (1967).
- <sup>11</sup>H. Yamada-Kaneta, *Solid State Phenomena* **82–84**, 87 (2002).
- <sup>12</sup>J. Kato, K. M. Itoh, H. Yamada-Kaneta, and H.-J. Pohl, *Phys. Rev. B* **68**, 035205 (2003).
- <sup>13</sup>P. G. Sennikov, T. V. Kotereva, A. G. Kurganov, B. A. Andreev, H. Niemann, D. Schiel, V. V. Emtsev, and H.-J. Pohl, *Semiconductors* **39**, 320 (2005).
- <sup>14</sup>H. Yamada-Kaneta, *Phys. Rev. B* **58**, 7002 (1998).
- <sup>15</sup>ASTM Standards, v.10.05, p. 438 (1996).
- <sup>16</sup>P. Becker, H.-J. Pohl, H. Riemann, and N. Abrosimov, *Phys. Status Solidi A* **207**, 49 (2010).
- <sup>17</sup>B. Gorshunov, A. Volkov, I. Spektor, A. Prokhorov, A. Mukhin, M. Dressel, S. Uchida, and A. Loidl, *Int. J. Infrared Millimeter Waves* **26**, 1217 (2005).
- <sup>18</sup>M. Dressel and G. Grüner, *Electrodynamics of Solids* (Cambridge University Press, Cambridge, 2002).
- <sup>19</sup>P. W. Milonni, *Fast Light, Slow Light and Left-Handed Light* (Institute of Physics Publishing, Bristol, Philadelphia, 2005).
- <sup>20</sup>C. Wurster, E. Dittrich, W. Scheitler, K. Lassmann, W. Eisenmenger, and W. Zulehner, *Physica B* **219–220**, 763 (1996).
- <sup>21</sup>U. Werling and K. F. Renk, *Phys. Rev. B* **39**, 1286 (1989).
- <sup>22</sup>A. A. Volkov, Yu. G. Goncharov, V. P. Kalinushkin, G. V. Kozlov, and A. M. Prokhorov, *Fiz. Tverd. Tela. (Leningrad)* **31**, 262 (1989) [*Sov. Phys. Solid State* **31**, 1249 (1989)].
- <sup>23</sup>A similar problem has been found previously in the case of Ge:O<sub>i</sub>: There the Ge-O-Ge complex has bent-molecule character, the lowest states of the 2D LEAE mode being rotational, showing an influence of the D<sub>3d</sub> crystal potential of the next-nearest Ge-neighbors,<sup>24</sup> i.e., a “direct” participation of two Ge partners to the oxygen motion of the lowest mode appears plausible.<sup>25</sup> If or if not, a host isotope effect has been measured by phonon spectroscopy in isotopically enriched <sup>70</sup>Ge, <sup>73</sup>Ge, <sup>74</sup>Ge, and <sup>76</sup>Ge (Refs. 26 and 27) with a linear dependence of the resonance positions on Ge mass and the position of the <sup>nat</sup>Ge resonance corresponding well to the average Ge mass. However, the line width measured in <sup>nat</sup>Ge:O<sub>i</sub>, though being about a factor of two larger than those of the qmi resonances, is by a factor of two smaller than what is estimated from the measured shifts and the occurrence of the Ge-isotopes. This may be regarded as an argument against a local host isotope effect. Since the position of the resonances in the 2D LEAE spectrum of <sup>nat</sup>Ge:O<sub>i</sub> fits well to the average-mass value, this has been alternatively interpreted as an averaging participation of a larger neighborhood or the lattice as a whole.
- <sup>24</sup>M. Gienger M. Glaser, and K. Laßmann, *Solid State Commun.* **86**, 285 (1993).
- <sup>25</sup>E. Artacho, F. Yndurain, B. Pajot, R. Ramirez, C. P. Herrero, L. I. Khirunenko, K. M. Itoh, and E. E. Haller, *Phys. Rev. B* **56**, 3820 (1997).
- <sup>26</sup>N. Aichele, U. Gommel, K. Laßmann, F. Maier, F. Zeller, E. E. Haller, K. M. Itoh, L. I. Khirunenko, V. Shakhovtsov, B. Pajot, E. Fogarassy, and H. Müssig, *Mater. Sci. Forum* **258–263**, 47 (1997).
- <sup>27</sup>K. Laßmann, C. Linsenmaier, F. Maier, F. Zeller, E. E. Haller, K. M. Itoh, L. I. Khirunenko, B. Pajot, and H. Müssig, *Physica B* **263–264**, 384 (1999).
- <sup>28</sup>Here we extrapolated from the 28–29 and 28–30 positions obtained in <sup>nat</sup>Si,<sup>11</sup> since to our knowledge there exists no measurement of this mode in a <sup>30</sup>Si crystal.
- <sup>29</sup>B. Pajot, E. Artacho, C. A. J. Ammerlaan, and J.-M. Spaeth, *J. Phys.: Condens. Matter* **7**, 7077 (1995).
- <sup>30</sup>K. Gaal-Nagy, M. Schmitt, P. Pavone, and D. Strauch, *Comput. Mater. Sci.* **22**, 49 (2001).
- <sup>31</sup>C. Ulrich, E. Anastassakis, K. Syassen, A. Debernardi, and M. Cardona, *Phys. Rev. Lett.* **78**, 1283 (1997).
- <sup>32</sup>H. Yamada-Kaneta, *Mater. Sci. Forum* **258**, 355 (1997).
- <sup>33</sup>M. Cardona and M. L. W. Thewalt, *Rev. Mod. Phys.* **78**, 1173 (2005).
- <sup>34</sup>M. D. McCluskey and E. E. Haller, *Phys. Rev. B* **56**, 9520 (1997); private communication of selected values of the fitting curve is gratefully acknowledged.
- <sup>35</sup>A. M. Stoneham, *Rev. Mod. Phys.* **41**, 82 (1969).
- <sup>36</sup>J. J. Wortmann and R. A. Evans, *J. Appl. Phys.* **36**, 153 (1965).
- <sup>37</sup>E. Sozontov, L. X. Cao, A. Kazimirov, V. Kohn, M. Konuma, M. Cardona, and J. Zegenhagen, *Phys. Rev. Lett.* **86**, 5329 (2001).
- <sup>38</sup>W. Scheitler, Ph.D. thesis, Universität Stuttgart, 1987.
- <sup>39</sup>H. Neubrand, *Phys. Status Solidi B* **90**, 301 (1978).
- <sup>40</sup>H. Zeile and K. Laßmann, *Phys. Status Solidi B* **111**, 555 (1978).
- <sup>41</sup>A. Ambrosy, Ph.D. thesis, Universität Stuttgart, 1987.
- <sup>42</sup>A. M. Stoneham, on a visit to the ultrasonic laboratory, suggested that the residual Gaussian might be due to the isotopic impurity of <sup>nat</sup>Si and the line shape due to the fact that at the relatively high concentrations of the <sup>29</sup>Si and <sup>30</sup>Si isotopes with high probability there are several isotopes within the large volume of the acceptor wave function, which might lead to a Gaussian narrowing of the observed line. Of course, at intermediate concentrations of point defects, a convolution of Gaussian and Lorentzian is obtained, as discussed by Neubrand.<sup>39</sup>
- <sup>43</sup>Also for the ν<sub>3</sub> mode of O-Ge-O, the analog to A<sub>2u</sub> in Si, a matrix-induced isotopic shift has been discussed.<sup>44</sup> Again, the isotopic changes of three-phonon DOS and of the lattice constant have been considered to explain for the observed shifts and broadenings for this mode.
- <sup>44</sup>B. Pajot, E. Artacho, L. I. Khirunenko, K. Itoh, and E. E. Haller, *Mater. Sci. Forum* **258–263**, 41 (1997).
- <sup>45</sup>The ratio for the <sup>nat</sup>Si-sample 1 is very small: 81.4. However, because of the large error bars (allowing nearly a factor of 1.5 from the average) due to its very low concentration of 5.7 × 10<sup>16</sup> cm<sup>-3</sup> should not enter here.